Pharm Res (2013) 30:1836–1847
DOI 10.1007/s11095-013-1027-2

RESEARCH PAPER

Caveolar Uptake and Endothelial-Protective Effects of Nanostructured Lipid Carriers in Acid Aspiration Murine Acute Lung Injury

Matina Kardara • Sophia Hatziantoniou • Aggeliki Sfika • Aliki G. Vassiliou • Elena Mourelatou • Christina Magkou • Apostolos Armaganidis • Charalambos Roussos • Stylianos E. Orfanos • Anastasia Kotanidou • Nikolaos A. Maniatis

Received: 8 October 2012 / Accepted: 12 March 2013 / Published online: 3 April 2013

ABSTRACT

Purpose Nanostructured lipid carriers (NLC), nanosized phospholipids/triglyceride particles developed for drug delivery, are considered biologically inactive. We assessed the efficacy of unloaded NLC as experimental treatment for acute lung injury (ALI).

Methods To induce ALI, C57Black/6 male mice received intratracheal injections of HCl or saline; A single dose of 16 mg/Kg NLC or saline was injected intravenously concomitantly with HCl challenge. NLC uptake mechanisms and effects on endothelial permeability and signaling were studied in cultured endothelial cells and neutrophils.

Results NLC pre-treatment attenuated pulmonary microvascular protein leak, airspace inflammatory cells, thrombin proteolytic activity and histologic lung injury score 24 h post insult. Using fluorescence measurements and flow cytometry in mouse lung microvascular endothelial cell culture homogenates, we determined that NLC rendered fluorescent by curcumin labeling are taken up by endothelial cells from mice expressing caveolin-1, the coat protein of caveolar endocytic vesicles, but not from caveolin-1 gene-disrupted mice, which lack caveolae. In contrast, conventional emulsions (CE), consisting of larger particles, were not incorporated. In addition, NLC pre-treatment of cultured human lung microvascular endothelial cells abrogated thrombin-induced activation of p44/42, albumin permeability response, actin cytoskeletal remodeling and interleukin-6 production. Finally, NLC but not CE abrogated lipopolysaccharide-triggered interleukin-8 release.

Conclusions NLC are engulfed by endothelial caveolae and possess endothelial-protective effects. These novel properties may be of potential utility in ALI.

KEY WORDS acute lung injury · extracellular-regulated kinase · nanomedicine · permeability · thrombin

ABBREVIATIONS

ALI	Acute lung injury
BAL	Broncho-Alveolar Lavage
CE	Conventional emulsions
FACS	Fluorescence-activated cell sorting
FITC-BSA	Fluorescein-isothiocyanate labelled bovine serum albumin
HPEMC-ST1	Human Pulmonary Microvascular Endothelial cells
IL-6	Interleukin-6

M. Kardara • A. Sfika • A. G. Vassiliou • A. Armaganidis • C. Roussos • S. E. Orfanos • A. Kotanidou • N. A. Maniatis
First Department of Critical Care Medicine & Pulmonary Services
GP Livanos and M Simou Laboratories, Evangelismos Hospital
Medical School of Athens University
Athens, Greece

C. Roussos • A. Kotanidou
1st Department of Critical Care and Pulmonary Services
"Evangelismos" Hospital Medical School of Athens University
Athens, Greece

S. E. Orfanos • N. A. Maniatis
2nd Department of Critical Care, "Attikon" Hospital
Medical School of Athens University
Athens, Greece

S. Hatziantoniou • E. Mourelatou
Department of Pharmaceutical Technology
School of Pharmacy of Athens University
Athens, Greece

C. Magkou
Department of Pathology, "Evangelismos" Hospital, Athens, Greece

N. A. Maniatis (✉)
Ploutarhou 3, 2nd Floor
Athens 10675, Greece
e-mail: nmaniatis@med.uoa.gr

It	Intratracheal
Iv	Intravenous
MLMVEC	Mouse Lung microvascular endothelial cells
NLC	Nanostructured lipid carriers
NS	Normal saline
PBS	Phosphate-buffered saline
PI	Polydispersity Index
RI	Real refractive index
SDS-PAGE	Sodium Dodecacyl Sulfate Polyacrylamide Gel Electrophoresis
WT	Wild-type

INTRODUCTION

Acute lung injury (ALI), a major cause of respiratory failure in critically ill patients, is associated with increased morbidity and mortality. A diffuse inflammatory response to a variety of insults, including infections, sepsis, multiple trauma, chemical irritants and toxins (1) leads to disruption of the alveolocapillary membrane and pulmonary edema due to endothelial hyperpermeability. Treatment is supportive and focuses mainly on addressing the inciting cause, while providing lung-protective mechanical ventilation, or, in refractory cases, applying rescue techniques of extracorporeal oxygenation and carbon dioxide removal. Despite these advances, ALI substantially complicates the clinical course of critically ill patients and prolonged intensive care unit stay is the norm. For these reasons it would be very useful to have a pharmacologic adjunct to supplement the host of interventions usually required for a positive outcome in these patients.

Nanostructured Lipid Carriers (NLC) are novel nanosized particles for drug delivery, which have evolved through efforts to maintain continuous drug levels in a desired range, while reducing unwanted effects by improving tissue or organ selectivity (2,3). They are part of a broader category of lipidic nanocarriers, along with liposomes, solid lipid nanoparticles and nanoemulsions (4–10). Even though they have initially been investigated for topical application in cosmetics and dermal therapeutics, successful systemic delivery has also been reported (11). NLC are prepared by biocompatible lipids and are considered biologically neutral when administered to unstimulated cells. However, little is known regarding their effects on diseased tissues and since they are sufficiently small to enter cells *via* standard macromolecular uptake organelles, including caveolar vesicles, they could plausibly influence cellular function. In this work we tested the utility of NLC in preventing pulmonary dysfunction in a mouse model of ALI induced by intratracheally-injected hydrochloric acid (HCl). Furthermore, we assessed the ability of NLC to be taken up by endothelial caveolae. Finally, we probed the effects of NLC on endothelial cells stimulated by thrombin, a potent vasoactive agent known to invoke disruption of the endothelial barrier.

MATERIALS AND METHODS

Antibodies and Reagents

All primary antibodies were purchased from Cell Signalling (Beverly, MA, USA) Horseradish peroxidase-conjugated goat anti-mouse IgG and goat anti-rabbit IgG were obtained from Santa Cruz Biotechnology (CA, USA). ProLong Gold antifade reagent with 4′,6-diamidino-2-phenylindole (DAPI) and Alexa Fluor 488 phalloidin were obtained from Invitrogen (Carlsbad, CA, USA). Egg Phosphatidylcholine (Lecithin EPC, Lipoid S-100), caprylic/capric triglycerides (Miglyol 812c, Crodamol GTCC (S), Lemmel, Spain), hydrogenated palm oil (Softisan 154, CONDEA, Witten, Germany), Polyethylene glycol-15-hydroxystearate (Solutol HS 15 BASF, Ludwigshafen, Germany), Curcumin (Acros Organics). All other reagents were purchased from Sigma-Aldrich (Irvine, United Kingdom), unless stated otherwise.

Preparation, Physicochemical Characterization and Stability Assessment of NLC

Nanostructured lipid carriers are prepared using the double emulsion technique (12). Briefly, the appropriate lipid mixtures (triglycerides, phosphatidylcholin,) and Solutol are diluted in dichloromethane and a small volume of deionized water is added. The mixtures are sonicated in a probe sonicator and deionized water is added to the primary emulsion. After sonication, a triple emulsion (w/o/w) is formulated. The sample is diluted to the final volume and the remaining organic solvent is evaporated under stirring in a water bath at 30–35°C for 30 min and under reduced pressure for another 30 min. The sample is stored at 4°C until further use (13,14). Curcumin loaded NLC were prepared for cellular uptake study, dissolving the appropriate amount of curcumin in the initial lipid mixture. The lipid content of the formulations was analyzed using HPTLC/FID (IATROSCAN MK5^{NEW} (Iatron Laboratories, INC. Tokyo, Japan) to determine the final ratio of the components and to assess the preparation procedure (15,16). Curcumin's concentration was determined by UV–vis spectroscopy at 423 nm (Pharmaspec UV-1700, Shimadzu, Japan) after passing the samples from a Sephadex G50 column to separate from NLC-incorporated curcumin. The calculation was achieved constructing a calibration curve of curcumin in methanol. Size distribution (mean particle diameter and ζ-potential) measurements were performed after preparation of the nanoparticles as follows: 1 mL of the nanoparticles dispersion was diluted in HPLC-grade water (pH 5.6–5.7) to 3 mL final volume, and *z*-average mean and ζ-potential were measured. Measurements were made at 633 nm, at a 90° fixed angle and 25°C, in a photon correlation spectrometer (Zetasizer 3000

HS_A, Malvern, UK) and analyzed by the CONTIN method (MALVERN software). The physical stability of the formulations over time is assessed by monitoring the size and ζ-potential of the formulations as described above after their preparation and at fixed time intervals (0, 7, 15, 40, 60, 180 days). All measurements were performed in three independent preparations

Preparation and Physicochemical Characterization of Conventional Emulsion

Conventional emulsion (CE) is prepared using similar quantities of ingredients to those used for NLC preparation. Briefly, the lipid phase (triglycerides, phosphatidylcholin, Solutol) and aqueous phase (deinonized water) are heated in separate beakers at 70°C. The emulsification is achieved by adding small volumes of distilled water under stirring. The emulsion is then cooled under constant stirring until it reaches room temperature and finally stored at 4°C until further use. Curcumin- loaded CE is prepared by adding the appropriate amount of curcumin in the initial lipid phase. The lipid content, curcumin's concentration of the formulations was determined as described for NLC formulations. Size distribution (mean particle diameter and ζ-potential) measurements were performed using laser diffraction (Mastersizer S, Malvern Instruments Ltd, Malvern, UK) fitted with a small volume sampler set at 50% of its speed capacity. The focal lens was 330 mm with a size range 0.5–880 μm. The background was measured after filling the stirrer with deionized water double-filtered through 220 nm filters. Aliquots of the samples were added to the stirrer until obscuration of approximately 20% is achieved. Each sample was measured in triplicate setting 2000 scans/run. The real refractive index (RI) was set at 1.456 and the imaginary RI at 0.01.

Mice

Ten- to fifteen-week-old C57/Black6 male mice weighing 25±2 g were purchased from the Biomedical Sciences Research Center 'Alexander Fleming', Vari, Greece. Mice were housed under veterinarian supervision at 20 to 22°C, 55±5% humidity, and a 12 h light–dark cycle; food and water were given *ad libitum*. All experimentation was approved by an internal Institutional Review Board of "Evangelismos" Hospital, as well as by the veterinary service of the local governmental Prefecture.

Experimental Groups and Treatments

To induce ALI, mice were exposed to intratracheal (*it*) 0.1N HCl. NLC was delivered as a single intraorbitally-applied intravenous (*iv*) injection at a dose of 16 mg/Kg administered immediately prior to *it* HCl ($n=12$) or saline (NS, $n=13$). Control groups received *it* NS with ($n=13$) or without *iv* NLC ($n=6$).

Lung Injury Protocol

Immediately following injection of NLC or NS, mice were anesthetized with intraperitoneal ketamine/xylazine (100/5 mg/kg), the trachea was exposed *via* median incision and 50 μL of HCl 0.1 N or NS were injected using a 500 μL syringe and 27-gauge needle. The incision was closed with continuous 3–0 silk suture. Twenty-four hours following *it* injection, mice were anesthetized with ketamine/xylazine, the inferior vena cava and abdominal aorta were transected and the mouse allowed to exsanguinate. Broncho-Alveolar Lavage (BAL) was performed by injecting and slowly aspirating three 0.5 mL aliquots of ambient-temperature-Phosphate-Buffered Saline (PBS) into the tracheal cannula. BAL fluid was separated from cellular components by centrifugation at 800*g* for 5 min at 4°C and stored at −80°C. Cells were resuspended in PBS and BAL total cell count and differential were obtained with a hemocytometer, and cytocentrifugation/May-Gruenwald-Giemsa stain, respectively. The chest was opened and the pulmonary circulation was flushed free of blood by slowly injecting 10 mL of PBS into the right ventricle. The right lung was then dissected lobe-by-lobe, the tissue fragments were rinsed with PBS, blotted dry on tissue paper and snap-frozen in liquid nitrogen. The left lung was then dissected and stored in 10% buffered formalin until processing.

Lung Injury Score

Grading of lung injury severity was performed by a blinded pathologist (CM) in haematoxylin-eosin 4 μm-thick paraffin-embedded lung tissue sections using a scale from 0 to 4 to evaluate the degree of interstitial inflammation, alveolar inflammation and alveolar septal congestion (17).

BAL Total Protein Determination

Total protein concentration in the BAL was determined with the Bio-Rad Dc Protein Assay kit (Bio-Rad Laboratories, Hercules, CA, USA) according to the manufacturer's instructions.

Thrombin Activity in BAL

For the measurement of thrombin activity, 50 μL of sample or standard dilutions of thrombin were added to 100 μL PBS and incubated with 50 μL chromogenic substrate S-2238 (5 mM, Chromogenix AB, Molndel, Sweden) at 37°C for 2 h. Addition of 50 μL of 20% acetic acid terminated the reaction and the absorbance at 405 nm was measured.

Cell Culture

Immortalized Human Pulmonary Microvascular Endothelial cells (HPMEC-ST1) (18), a generous gift from Vera Krump-Konvalinkova, University of Munich, Germany, were cultured in M199 medium supplemented with 20% fetal bovine serum (FBS), Glutamax (2 mM), Penicillin/Streptomycin (100 U/100 g/mL, all Invitrogen), sodium heparin (25 μg/mL), and endothelial growth factor supplement (ECGS, 50 mg/mL). Mouse Lung microvascular endothelial cells (MLMVECs) isolated from wild-type (WT) and Caveolin-1 knockout (Cav-$1^{-/-}$) mice, kindly provided by Dr. Richard D. Minshall, Department of Pharmacology, University of Illinois at Chicago, USA, were grown in Dulbecco's Modified Eagle Medium/Ham's F-12 base, 10% FBS, Penicillin/Streptomycin (100 U/100 g/mL), glutamine (2 mM), ECGS (50 g/ml) and vascular endothelial growth factor (VEGF, 20 ng/mL). All cells were serum-starved for 2 h prior to each experiment.

Transendothelial Permeability Assay

Cultured HPMEC-ST1 were seeded on microporous polyethylene terephthalate membranes (Transwell, pore size 1. 0 μm, diameter 6.5 mm, Millipore, Billerica, MA, USA) (2×10^4 cells/well) and grown for 4 days to attain confluence. The luminal (upper) and abluminal (lower) chambers contained 0.2 mL and 0.8 mL growth medium, respectively. Endothelial monolayers were washed and placed in growth-arresting medium (DMEM/Ham's F-12 supplemented with 1% BSA). Cells were subsequently incubated with different concentrations of NLC (0.033, 0.33 and 3.3 π.μ.) for 30 min prior to the addition of thrombin (1 U/mL, Calbiochem, USA) and fluorescein-isothiocyanate-labelled albumin (FITC-BSA) at a concentration of 1 mg/mL was added in the upper chamber of the well. Samples were collected from the lower chamber after 1 h and fluorescence was measured on a fluorescence microplate reader (Tecan GENios, Männedorf, Switzerland) using excitation and emission filters set at 480 and 520 nm, respectively. Albumin permeability is expressed as μg FITC-BSA/mL/min.

Immunofluorescence Staining and Microscopy

For immunofluorescence staining, HPMEC-ST1 cells were grown to confluence on gelatin-coated glass coverslips, serum-starved for 2 h in growth-arresting medium and incubated with NLC (3 mg/mL) or medium for 30 min prior to addition of thrombin (1 U/mL). Cells were then washed with acid buffer (0.2 M acetic acid, 0.5 M NaCl, pH 2.5) to remove unbound tracer, fixed with 2% paraformaldehyde for 10 min, permeabilized in 1% Triton X-100, blocked with 1% ovalbumin for 20 min and stained with Alexa Fluor 488 phalloidin in 1% ovalbumin for 20 min. Coverslips were then washed and mounted on glass slides with Prolong DAPI. An Eclipse E600 (Nikon, Tokay, Japan) immunofluorescence microscope was used for viewing the preparations.

Immunoblotting

Cells were washed with cold PBS, lysed with lysis buffer (50 mM Tris–HCl, pH 7.5, containing 150 mM NaCl, 1 mM EDTA, 0.25% sodium deoxycholate, 1% IGEPAL, 0.1% SDS, 1 mM Na_3VO_4, 1 mM NaF, 44 g/mL phenylmethylsulfonyl fluoride, and protease inhibitor mixture) and insoluble materials were removed by centrifugation (14,000×*g* for 15 min). Supernatants were collected and the protein concentration was measured with Biorad DC protein assay (Biorad, Hercules, CA, USA). Samples (15–30 μg) were analyzed by SDS-PAGE, transferred to polyvinylidene fluoride membranes (Millipore, Billerica, MA, USA) and incubated in 5% dry milk in Tris-buffered saline with Tween 20 for 1 h at ambient temperature. Membranes were probed with the appropriate primary antibody overnight at 4°C and with horseradish peroxidase-conjugated secondary antibody for 1 h at ambient temperature. Proteins were detected using an ECL kit (Pierce, Rockford, lL, USA). Densitometric analysis of the films was performed with the Image J analysis software (National Institutes of Health, Bethesda, MD, USA).

Cellular Uptake of NLC

Cellular uptake of nanoparticles was studied using confluent mouse and human LMVECs incubated for 1 h with NLC-loaded curcumin (3 mg/mL) or NLC- and CE- loaded curcumin (1 mg/mL) for 0.5, 1 and 2 h respectively. After treatment, cells were washed to remove cell surface-bound tracer with acid buffer and ice-cold HBSS. For microscopy, cells were cultured on gelatin-coated glass coverslips, washed, fixed with 2% paraformaldehyde for 10 min and mounted as described. For fluorescence-activated cell sorting (FACS) analysis, the washed cells were collected in HBSS and FACS analysis was performed with 5×10^4 cells/sample, using BD FACScalibur flow cytometer and CellQuest Pro software (BD Biosciences, CA, USA). Additionally, washed cells were lysed in lysis buffer, centrifuged (14,000×*g* for 15 min) and the lysate's fluorescence was measured on a fluorescence microplate reader as described. Curcumin uptake was expressed in Relative Fluorescense Units/μg protein and μg Curcumin/μg protein.

Quantification of Human IL-6 and IL-8 by ELISA

Human Pulmonary Microvascular Endothelial cells-ST1 were grown to confluence, growth-arrested in M199 with 0.1% BSA for 2 h and pretreated with NLC (3 mg/mL) for

30 min and thrombin (1 u/mL) for 0, 90 and 120 min. Supernatants were used for the quantification of Human IL-6 using a DuoSet ELISA kit (R&D, Minneapolis, MN, USA) according to manufacturer's instructions.

Healthy blood donor neutrophils were obtained from freshly drawn peripheral blood by dextran sedimentation and hypotonic lysis of residual erythrocytes, followed by centrifugation on Ficoll-Hypaque (Amersham Biosciences AB, Sweden). Cells were resuspended in HBSS, plated in 12 well plates (2×10^5 cells/well) and treated with or without lipopolysaccharide (LPS) from *P. aeruginosa* 10 (100 ng/mL) and NLC or CE (2 mg/mL) for 3 h. Supernatants were used for the quantification of Human IL-8 as described above.

Data Analysis

Data are presented as mean ± SD. Statistical hypothesis testing was undertaken using one-way ANOVA with Student-Neumal-Keuls post-hoc tests or two-way ANOVA (GraphPad Prism version 5.00 for Windows, GraphPad Software, San Diego California USA, www.graphpad.com). A p-value <0.05 was considered significant.

RESULTS

Lipid Content, Particle Size Measurements and Physico-chemical Stability Assessment of NLC

The lipid content of NLC dispersion was measured at 33.4 mg/mL, of which EPC: 16.66 mg/mL and triglycerides (Softican + Miglyol): 16.76 mg/mL while curcumin's concentration was 1.45 ± 0.19 mg/mL. Particle size and ζ-potential distribution study revealed a mean particle size of 61.3 nm ± 0.3, Polydispersity Index (PI): 0.113, while ζ- Potential was −19.1 mV ± 2.8 and Width was 11.4. The Stability study shows that the mean particle size and ζ-potential distribution is maintained stable for at least 6 months (Fig. 1)

Lipid Content, Particle Size Measurements and Physico-chemical Stability Assessment of Conventional Emulsion

The lipid content of CE dispersion was measured at 29.7 mg/mL, of which EPC: 14.8 mg/mL and triglycerides (Softican + Miglyol): 14.9 mg/mL while curcumin's concentration was 8.7 ± 0.09 mg/mL. Particle size distribution study revealed: Mean hydrodynamic diameter: 10.3 μm ±0.2, Span: 1.5. The stability study shows that the mean particle size is maintained stable for 1 month (not shown).

NLC Reduce Inflammation, Permeability and Coagulation in Experimental Lung Injury

We used a preclinical model of ALI caused by *it* injection of HCl to explore biologic effects of NLC. Treatment comprised *iv* administration of NLC immediately preceding HCl injection, while the reference group received NS. Animals were sacrificed 24 h later and typical readouts of ALI were recorded, including BAL cellularity and total protein, in addition to thrombin proteolytic activity. As shown in Fig. 2a, endotracheal exposure to HCl is associated with an inflammatory response characterized by airspace infiltration, mostly with neutrophils (Fig. 2b). In comparison, BAL fluid from mice pretreated with NLC contained reduced numbers of total cells and neutrophils (Fig. 2a, b). Since pulmonary microvascular permeability is typically increased in ALI models, we measured BAL total protein as a marker of pulmonary endothelial integrity. Contrary to mice receiving placebo, which responded to *it* HCl with a significant protein leak in the airspace, endothelial barrier was preserved in NLC-pretreated mice (Fig. 2c). Finally, we measured BAL thrombin activity as a marker for the activation of the coagulation cascade, which is known to occur in the airspace compartment in ALI. We found increased thrombin proteolytic activity in BAL fluid from HCl-challenged mice, but this was significantly attenuated by NLC (Fig. 2d).

NLC Preserve Lung Micromorphology in ALI

Microstructural lesions in lung tissue were characterized in hematoxylin-eosin stained lung sections using a previously reported composite score (17). Injection of HCl elicited patchy, dense mononuclear infiltrates, alveolar thickening and airspace collapse (Fig. 3), consistent with increased-permeability edema in the setting of an acute inflammatory process and leading to raised lung injury scores ($p<0.05$ for comparison to *it* injection of NS, Fig. 3). These alterations were attenuated by NLC pre-treatment ($p<0.01$ for comparison with NS-HCl, Fig. 3). No microstructural lesions were noted with administration of NLC in mice receiving *it* NS.

Caveolin-1 is Required for Cellular Uptake of NLC

An important question regarding the mechanism of biological action of NLC is whether they act by binding on cell surface receptors or they are taken up by cells and exert actions within the cytoplasm. We began to approach this by incubating cultured MLMVEC cells with fluorescent NLC and measuring fluorescence intensity in the cell homogenate as a surrogate for the uptake of NLC (Fig. 4). NLC were rendered fluorescent by loading with curcumin. We found increased fluorescence intensity upon addition of NLC to cells, consistent with cellular internalization (Fig. 4a). Using

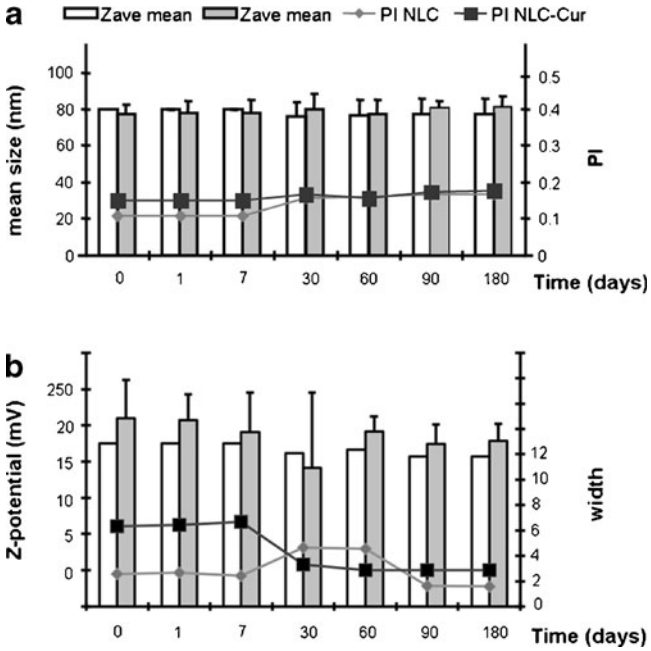

Fig. 1 Stability assessment of nanostructured lipid carriers. Measurement of mean size (nm) (**a**) and ζ-potential (mV) (**b**) of NLC for 6 months. The incorporation of curcumin in NLC does not affect the particle size and ζ-potential of the NLC. Both formulations (NLC and curcumin loaded-NLC) retained their physicochemical characteristics for at least 6 months. Zave: Z-average.

FACS analysis, we determined that roughly 10% of the cells had incorporated enough NLC to yield measurable levels of fluorescence (Fig. 4b). We next addressed the role of caveolar vesicles in the internalization of NLC. In cells devoid of caveolin-1, which are known to lack caveolae, uptake of NLC was diminished in all three procedures used, including fluorescence measurement of cell homogenates, FACS analysis and fluorescent microscopy (Fig. 4a, b, c).

Effect of Size on Cellular Uptake of Particles

To address the effect of size on particle uptake kinetics, we generated a lipid formulation comprising identical chemical components with NLC but larger particle size (diameter approximately 10 μm). We incorporated curcumin in the dispersed particles as a marker to compare uptake kinetics by HPMEC-ST1 cells for up to 120 min (Fig. 5). A time-dependent increase in uptake of NLC was observed, which reached a plateau at 60 min. In contrast, uptake of CE by the same endothelial cells was significantly lower (Fig. 5)

Endothelial Monolayer Protection by NLC

Since endothelial barrier leakiness is a critically important initial step in alveolar edema formation, we explored the effect of NLC using a system of HPMEC-ST1 cultured on microporous filters and challenged with thrombin to induce endothelial permeability (19), measured as accelerated flux of FITC-labelled albumin across the cell layer. Incubation

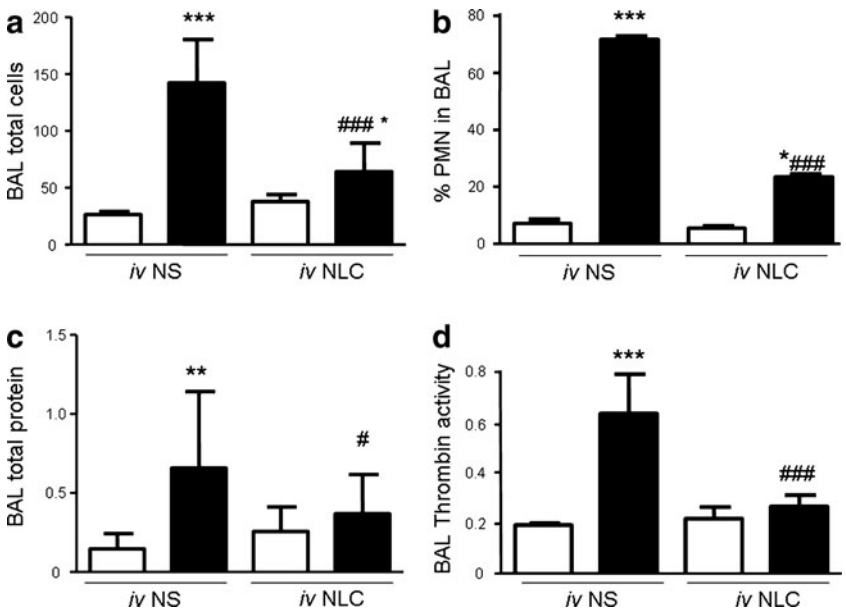

Fig. 2 Nanostructured lipid carriers for prevention of lung injury in HCl-challenged mice. To induce acute lung injury, mice were intratracheally (*it*) exposed to 0.1 N HCl (*black bars*) immediately prior to single intravenous (*iv*) injection of nanostructured lipid carriers (NLC) at a dose of 16 mg/Kg ($n = 12$) or saline (NS, $n = 13$). Control groups (*white bars*) received *it* injections of NS with or without *iv* NLC ($n = 13$ and 6, respectively). (**a**) Total bronchoalveolar lavage (BAL) cell count in cells/μL of BAL fluid was obtained by hemocytometer. (**b**) Neutrophil fraction of cytocentrifuged, May-Gruenwald-Giemsa-stained BAL cells. (**c**) Total protein in BAL samples measured by bicinchoninic acid reaction and expressed in μg/μL of BAL fluid. (**d**) Thrombin proteolytic activity in BAL measured as cleavage rate of chromogenic substrate S-2238 and expressed as Units/mL. *, # denote $p < 0.05$, **, ## denote $p < 0.01$, ***, ### denote $p < 0.001$ by one-way ANOVA with Neuman-Keuls post-hoc test; * stands for comparisons with *it* NS/*iv* NS; # for comparisons with *it* HCl/iv NS.

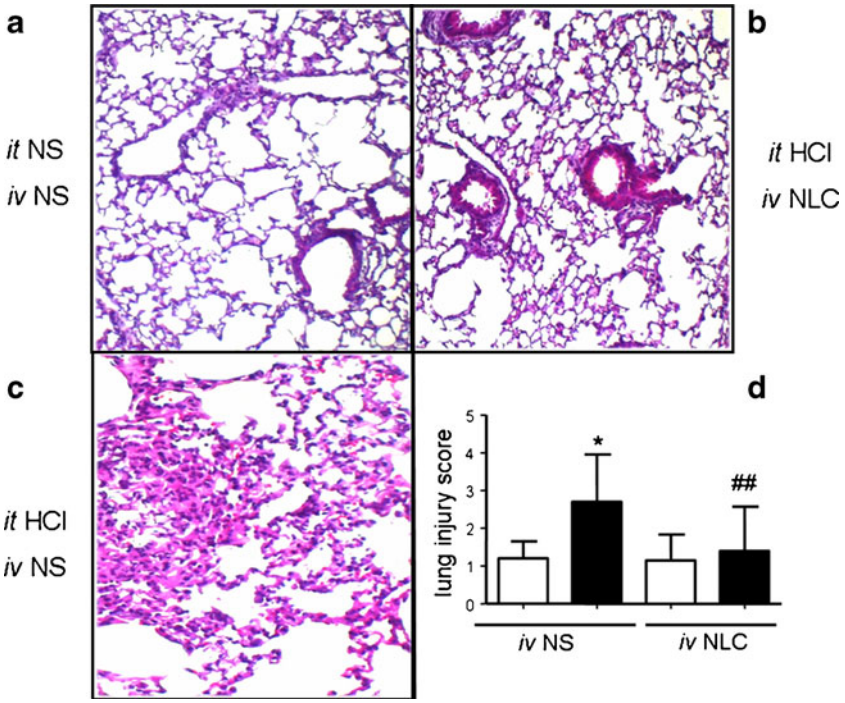

Fig. 3 Nanostructured lipid carriers and histological alterations in lungs of mice following intratracheal HCl injection. (**a**–**c**) Five μm-thick hematoxylin-eosin stained lung sections of mice challenged with HCl (*black bars*) or saline (NS-*white bars*) in the presence and absence of nanostructured lipid carriers (NLC). (**d**) Histological composite lung injury score comprising blinded grading for interstitial inflammation, alveolar inflammation and alveolar septal congestion on a scale from 0 to 4. *, # denote $p < 0.05$, **, ## denote $p < 0.01$, ***, ### denote $p < 0.001$ by one-way ANOVA with Neuman-Keuls post-hoc test; * stands for comparisons with intratracheal NS/intravenous NS; # for comparisons with intratracheal HCl/intravenous NS; *iv*: intravenous.

with NLC abrogated this effect and preserved endothelial continuity in a dose-dependent manner (Fig. 6). No measurable effect was observed by incubating cells with NLC alone.

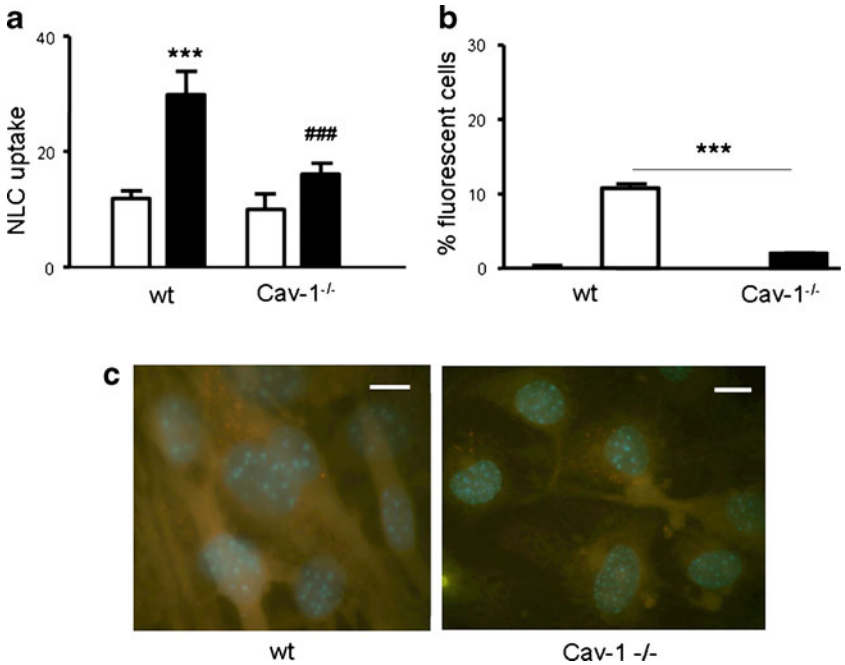

Fig. 4 Uptake of curcumin-loaded nanostructured lipid carriers by endothelial caveolae. (**a**) Lung microvascular cells from wild-type (WT) and caveolin-1 knockout (Cav-1$^{-/-}$) mice were incubated with curcumin-loaded (for fluorescence) nanostructured lipid carriers (NLC) at a concentration of 3.3 mg/mL for one hour (*black bars*) and fluorescence was measured in cell homogenate. Fluorescence levels of untreated (control) cells are represented by the *white bars*. NLC uptake is expressed as relative fluorescence units/μg protein of cell homogenate. (**b**) Same experiment as in "A" but uptake of NLC was measured by flow cytometry and expressed as percentage of fluorescent cells relative to all cells. (**c**) Cells were grown on glass coverslips, incubated with fluorescent NLC, fixed and studied under fluorescent microscope with 1,000× magnification. *, # denote $p < 0.05$, **, ## denote $p < 0.01$, ***, ### denote $p < 0.001$ by one-way ANOVA with Neuman-Keuls post-hoc test; * stands for comparisons with WT control (no NLC); # for comparisons with WT-NLC; $n = 3$ experiments.

NLC Modulate Actin Cytoskeletal Response to Thrombin

In the presence of thrombin, actin cytoskeletal remodelling and endothelial cell contraction occur, leading to junctional disruption and leakiness of the endothelial layer. Polymerized actin stained in quiescent HPMEC-ST1 with FITC-phalloidin is primarily distributed in the cell periphery (Fig. 7a, b). A shift in this arrangement is noted upon thrombin stimulation, marked by the appearance of thick actin cables (Fig. 7c). Addition of NLC in the cell-culture medium prevented actin cytoskeletal rearrangement and intercellular gap formation, in line with the protective effect noted in the albumin permeability studies.

NLC Interfere with Endothelial Signal Transduction and Cytokine Production

We sought to determine whether the observed protection against thrombin-induced barrier disruption in the *in vitro* model described above was attributed to effects of NLC on thrombin signaling pathways or to non-specific thrombin destruction. To this end, we initially tested thrombin proteolytic activity with the colorimetric assay described in "Materials and Methods" and found that it was retained in the presence of NLC (not shown), indicating that the observed effects were not due to repression of thrombin by NLC in the cell culture supernatant. We therefore proceeded to evaluate thrombin-induced p44/42 phosphorylation, one of the early signal relay stations in the thrombin cascade, in cultured HPMEC-ST1 using semi-quantitative immunoblotting. The strong and rapid activation of p44/42 by thrombin was practically abrogated by NLC (Fig. 8a, b). To determine the role of p44/42 in the thrombin permeability response, we blocked this pathway in cultured HPMEC-ST1 with UO126. This compound prevented ($p<0.05$) thrombin from increasing permeability and preserved the integrity of the endothelial barrier (Fig. 8c). Finally, since binding of various vasoactive agents on endothelial cells induces transcription of pro-inflammatory genes, we explored the effect of NLC on the induction of IL-6, a major component of the complex network of the innate immune response. Challenge of HPMEC-ST1 with thrombin elicited robust, time-dependent IL-6 induction (Fig. 8d), which could be significantly blunted by NLC supplementation ($p<0.001$ for the 90- and 120 min time-points, Fig. 8d).

NLC Blunt Lipopolysaccharide-Triggered Interleukin-8 Production by Neutrophils

Neutrophil activation leading to parenchymal cell damage is a principal factor of ALI pathogenesis and preventing neutrophil degranulation frequently reduces the severity of experimental ALI. We therefore tested the effect of NLC on the response of neutrophils to a challenge with LPS, a component of the cell wall of Gram negative bacteria and potent stimulant of immune cells (Fig. 9). Incubation of human neutrophils with LPS triggered a marked shedding of IL-8 in the cell culture medium. In the presence of NLC, however, IL-8 production was suppressed (Fig. 9). Conventional emulsion had no effect on IL-8 production, indicating that at this particle size no entry into neutrophils can be expected.

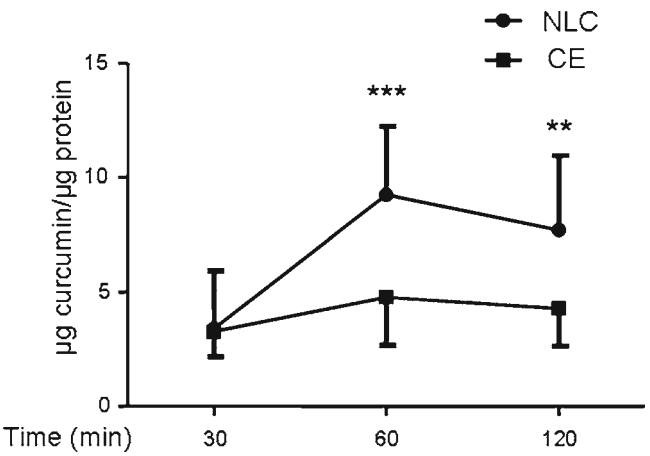

Fig. 5 Size-dependence of lipid particle cellular uptake kinetics. Human lung microvascular endothelial cells ST-1 were incubated with curcuming-tagged nanostructured lipid carriers (NLC) or conventional emulsion (CE) for the indicated time-points. Fluoresence of cell lysate is used to assess the amount of incorporated particles. ** denote $p<0.01$, *** denote $p<0.001$ by two-way ANOVA. The results represent pooled values from three separate experiments ($n=10$ wells/time-point).

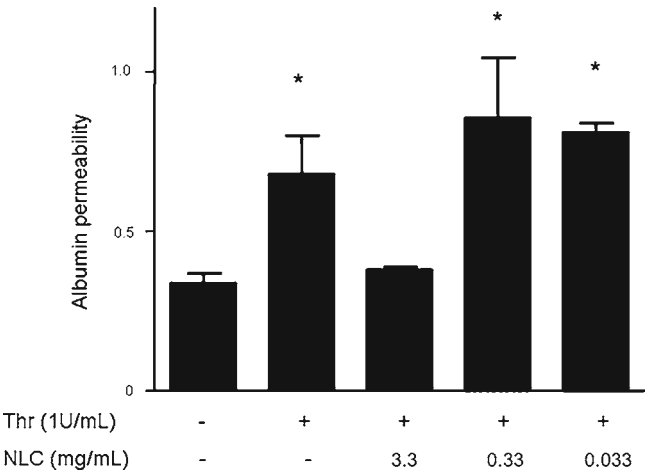

Fig. 6 Nanostructured lipid carriers oppose permeability-enhancing effect of thrombin. Human lung microvascular endothelial cells ST-1 were cultured on microporous filters and challenged with thrombin (Thr) 1 U/mL in the absence and presence of three different concentrations of nanostructured lipid carriers. The rate of fluorescein-isothiocyanate-labeled albumin (FITC-BSA) tracer flux in μg/mL/min is a marker of monolayer permeability. * denotes $p<0.05$ by one-way ANOVA with Neuman-Keuls post-hoc test for comparisons with FITC-albumin permeability of unstimulated cells (*left bar*), $n=3$ experiments.

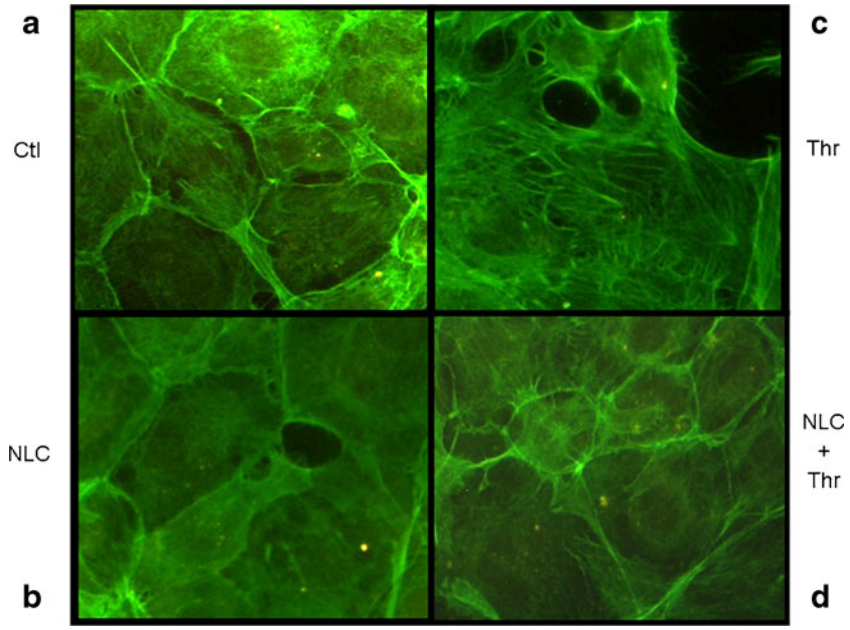

Fig. 7 Effect of nanostructured lipid carriers in actin cytoskeletal remodelling in response to thrombin. Human lung microvascular endothelial cells ST-1 grown on glass coverslips were challenged with 1 mg/mL of thrombin (thr) or cell culture medium (Ctl) in the presence and absence of nanostructured lipid carriers (NLC) at a concentration of 3.3 mg/mL. Cells were subsequently stained for polymerized actin using Alexa Fluor 488 phalloidin and observed with fluorescent microscope (1,000×).

DISCUSSION

Since recognition of the pathogenetic role of endothelial dysfunction in ALI, several promising experimental strategies have been proposed. Even though none has established itself into clinical practice to-date, the prospect of an agent with the capacity to reverse vascular leak and protect the endothelium remains exciting. In this context,

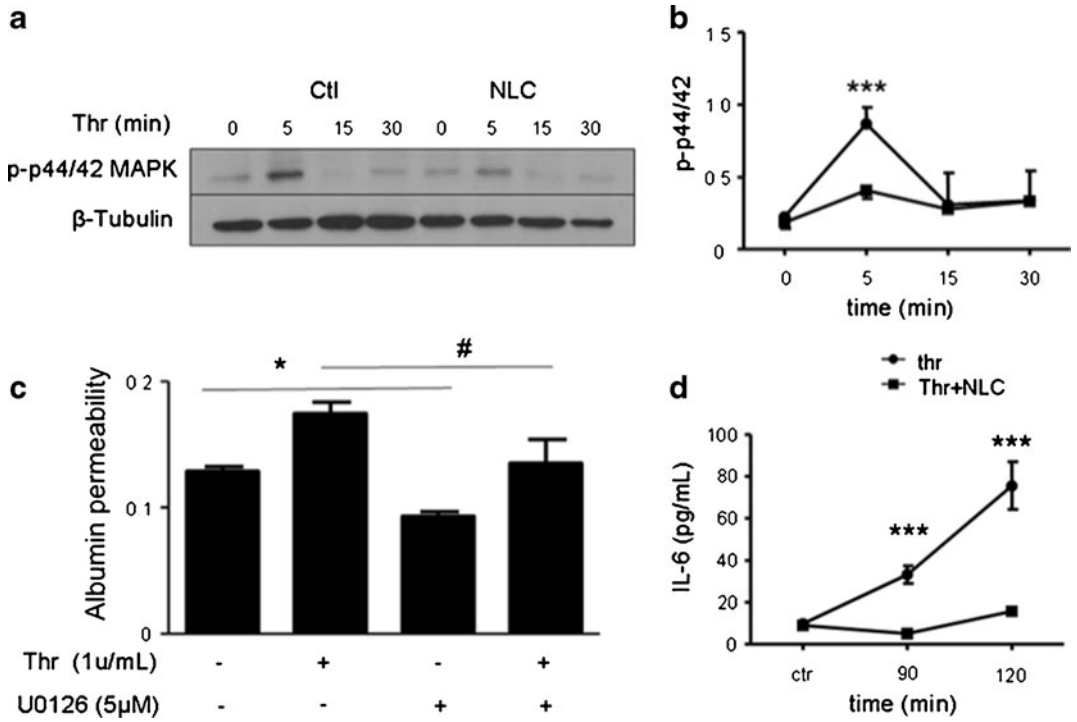

Fig. 8 Nanostructured lipid carriers disrupt thrombin signaling. (**a**) Human lung microvascular endothelial cells-ST1 were challenged with thrombin (thr) and phosphorylation of p44/42 kinase at Thr^{202}/Tyr^{204} was probed in the cell homogenate by immunoblotting. (**b**) Activation status of p44/42 expressed relative to β-tubulin in arbitrary units obtained by densitometric analysis. (**c**) Endothelial cells grown on microporous filters were challenged with thrombin 1 U/mL to increase albumin permeability in the presence and absence of p44/42 inhibitor. (**d**) Incubation of cells with thrombin for the indicated time-points with or without nanostructured lipid carriers and levels of interleukin-6 in the cell culture supernatant. * denotes $p < 0.05$, ** denote $p < 0.01$, *** denote $p < 0.001$ by two-way ANOVA for comparison with control, $n = 3$ experiments.

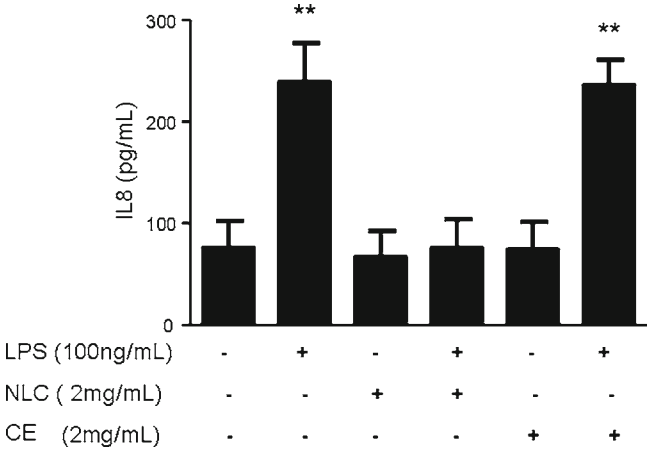

Fig. 9 Nanostructured lipid carriers exert actions on neutrophils. Human neutrophils were incubated with *P. aeruginosa* lipopolysaccharide (LPS) at a concentration of 100 ng/mL or plain medium to stimulate production of interleukin-8 (IL-8). Comparisons are drawn between the effects of NLC, conventional emulsion (CE) and plain medium. ** denote $p < 0.01$ by one-way ANOVA for comparison with control, data from $n = 2$ experiments were pooled.

we have investigated the utility of NLC, primarily known as vehicles for delivery of chemical compounds or genes into the lung, as a treatment for ALI. According to our data, the particles themselves, when administered at sufficiently high dose preserve pulmonary vascular integrity, modulate the innate immune response and may therefore have a place as a treatment for ALI. Moreover, our analyses show that NLC possess attributes important to modern therapeutic agents, including physicochemical stability for relatively prolonged periods, ease of storage and affordable production cost.

NLC are nanosized particles prepared by dispersing a phospholipid/triglyceride mixture (1:1 by weight) in an aqueous medium under specific conditions. A layer of phosphatidylcholine, an amphiphilic molecule composed of a lipidic polar headgroup and a non-polar lipidic-hydrocarbon chain, surrounds the core of the nanoparticles, formed by triglycerides arranged in a crystalline structure. The hydrophilic head group of phosphatidylcholin is directed toward the aqueous external medium and the hydrocarbon chains towards the lipophilic core.

Even though approximately two decades have passed since the discovery of NLC, most of the research has focused on topical application of drugs and relatively little is known regarding systemic delivery (11). Since these agents are considered biodegradable and devoid of biologic effects, their therapeutic potential has remained largely unexplored. We addressed this question using a mouse model of ALI provoked by aspiration of HCl. This chemical pneumonitis models some features of the clinical entity of ALI from gastric acid aspiration, a direct pulmonary insult from a chemical irritant (20,21), which may or may not contain bacteria. Nonetheless, its key pathogenetic features, most notably endothelial dysfunction, airspace inflammation and epithelial damage, are shared by most other forms of ALI.

In this experimental system, we observed that HCl instillation in the trachea elicited a patchy inflammatory reaction with substantial airspace infiltration by neutrophils, pulmonary vascular leak and initiation of coagulation. Intravenously injected NLC at the time of intratracheal HCl, however, suppressed airspace infiltration, consistent with an immunomodulatory effect. In addition, NLC prevented breakdown of the pulmonary vascular barrier and alveolar protein leak. The blunted thrombin proteolytic activity found in BAL fluid in NLC-treated mice suggests decreased intraalveolar coagulation. Not surprisingly, NLC significantly ameliorated micromorphological alterations in the lung.

To understand the mode of action of NLC in experimental ALI, we tested for endothelial engulfment of NLC, to suggest that they exert their effects from an intracellular location. Based on their diameter of 100 nm or less, a plausible route of entry would be through caveolar vesicles, which are known to incorporate albumin-conjugated particles of sufficiently small size to fit within caveolae (22). We thus delivered NLC to lung endothelial cells isolated from WT and caveolin-$1^{-/-}$, which are devoid of caveolae. In cells lacking caveolae, NLC incorporation was abrogated, as measured by flow cytometry, total fluorescence of cell homogenates and fluorescent microscopy, implying that caveolae may be a major vesicular carrier for NLC endocytosis. However, the mechanism of NLC entry into caveolae, e.g. *via* binding to a receptor or affinity to a membrane lipid, remains to be elucidated. Furthermore, it is unclear if NLC penetrate cells exclusively by these vesicles or, depending on cell type, other endocytic organelles. Detailed understanding of NLC uptake mechanisms could be exploited to improve cell penetration of medicines, genes or inhibitory RNA for the purposes of genetic manipulation. Modifications likely to enhance caveolar uptake of NLC would be a reduction in size (22) and specific targeting with the aid of caveolar markers (23). The former hypothesis is supported by the observation that, by increasing the size of the particles and keeping the chemical composition the same, cellular uptake is significantly lower. Therefore, a relationship between particle size and cellular permeability seems to exist.

We addressed endothelial-protective mechanisms of NLC using cultured human lung endothelial cells. For permeability assays, cells were cultured on microporous filters, which allow measurement of transendothelial flux of albumin in the absence of significant hydrostatic and oncotic pressure gradients. Stimulation of these cells with thrombin results in actin cytoskeletal polymerization, which exerts centripetal force on interendothelial junctions resulting in failure of the endothelial barrier. The presence of NLC in the culture medium opposed the rise in permeability, not by neutralizing thrombin, since thrombin enzymatic activity was maintained, but by modulating thrombin signalling, supported by the finding of

reduced p44/42 phosphorylation. To determine the role of p44/42 in the permeability response, we conducted a blocking experiment using UO126, which underscored the involvement of this system. The implication of these results is that NLC interferes with thrombin-activated pathways relevant to endothelial permeability by an unknown mechanism. However, a relationship to caveolin-1-dependent pathways cannot be excluded. It is possible that enrichment of NLC engulfed in caveolar compartments dismantles caveolin-1-dependent signaling pathways, which are known to assemble on the surface of caveolae (24). Finally, depressed IL-6 release from endothelial cells in response to thrombin is probably also related to alterations of intracellular signal relay by NLC.

The effects of NLC do not seem specific to endothelial cells; rather, neutrophils also respond to NLC by a reduction in LPS-triggered IL-8 production. In contrast, IL-8 production was unaffected by CE, indicating that only smaller particles can permeate the cells, at least within the timeframe of the experiment. The effect of NLC on neutrophils may comprise reduced bactericidal potency and immunosuppression or positive modulation of excessive neutrophil activation associated with lung damage in ALI.

A number of lipid preparations currently used in critical care have been shown to have biologic effects in animal and human studies, most notably lipid emulsions used as vehicles for delivery of propofol and other drugs in addition to lipid formulations used for parenteral nutrition (25,26). However, propofol at high doses may cause multi-organ dysfunction (27). With regard to parenteral nutrition, these mixed lipids may trigger synthesis of both pro- as well as anti-inflammatory mediators of the prostaglandine/leucotriene classes, so optimal composition is evolving (28). In contrast, NLC comprise chemically different compounds, which would predict a different mechanism of action and biosafety profile. It may thus be worthwhile to apply this preparation in different lung injury models and animal species, in order to test whether it may truly be a viable adjunct in the treatment of this devastating condition.

CONCLUSION

We propose that NLC are incorporated into cells *via* caveolar vesicles and counteract the effects of angiogenic agents. These properties are of possible value for the treatment of acute lung injury and pulmonary drug and gene delivery.

ACKNOWLEDGMENTS AND DISCLOSURES

This study was funded by an American Thoracic Society/Sepsis Alliance Research Grant and by the "THORAX" Research Center for Intensive and Emergency Thoracic Medicine, Athens, Greece

The preparation and characterization of NLC and CE formulations was performed at the Laboratory of Pharmaceutical Technology, Dept of Pharmacy, National and Kapodistrian University of Athens, Greece, under the kind hospitality of Professor C. Demetzos.

REFERENCES

1. Donahoe M. Acute respiratory distress syndrome: a clinical review. Pulm Circ. 2011;1:192–211.
2. Kolhe P, Misra E, Kannan RM, Kannan S, Lieh-Lai M. Drug complexation, *in vitro* release and cellular entry of dendrimers and hyperbranched polymers. Int J Pharm. 2003;259:143–60.
3. Langer R. Drug delivery and targeting. Nature. 1998;392:5–10.
4. Yang XY, Li YX, Li M, Zhang L, Feng LX, Zhang N. Hyaluronic acid-coated nanostructured lipid carriers for targeting paclitaxel to cancer. Cancer Lett. 2012, Jul 7 [Epub ahead of print].
5. Liu R, Liu Z, Zhang C, Zhang B. Nanostructured lipid carriers as novel delivery system for mangiferin: improving *in vivo* ocular bioavailability. J Pharm Sci. 2012;101:3833–44.
6. Alam MI, Baboota S, Ahuja A, Ali M, Ali J, Sahni JK. Intranasal administration of nanostructured lipid carriers containing CNS acting drug: pharmacodynamic studies and estimation in blood and brain. J Psychiatr Res. 2012;46:1133–8.
7. Zhen G, Hinton TM, Muir BW, Shi S, Tizard M, McLean KM, *et al.* Glycerol monooleate based nanocarriers for siRNA delivery *in vitro*. Mol Pharm. 2012. Jul 16 [Epub ahead of print].
8. Haque S, Md S, Alam MI, Sahni JK, Ali J, Baboota S. Nanostructure-based drug delivery systems for brain targeting. Drug Dev Ind Pharm. 2012;38:387–411.
9. Angelova A, Angelov B, Mutafchieva R, Lesieur S, Couvreur P. Self-assembled multicompartment liquid crystalline lipid carriers for protein, peptide, and nucleic acid drug delivery. Acc Chem Res. 2011;44:47–56.
10. Das S, Chaudhury A. Recent advances in lipid nanoparticle formulations with solid matrix for oral drug delivery. AAPS PharmSciTech. 2011;12:62–76.
11. Joshi MD, Muller RH. Lipid nanoparticles for parenteral delivery of actives. Eur J Pharm Biopharm. 2009;71:161–72.
12. Garcia-Fuentes M, Alonso MJ, Torres D. Design and characterization of a new drug nanocarrier made from solid–liquid lipid mixtures. J Colloid Interface Sci. 2005;285:590–8.
13. Deli G, Hatziantoniou S, Nikas Y, Demetzos C. Solid lipid nanoparticles and nanoemulsions containing ceramides: preparation and physicochemical characterization. J Liposome Res. 2009;19:180–8.
14. Hatziantoniou S, Deli G, Nikas Y, Demetzos C, Papaioannou GT. Scanning electron microscopy study on nanoemulsions and solid lipid nanoparticles containing high amounts of ceramides. Micron. 2007;38:819–23.
15. Hatziantoniou S, Demetzos C. Qualitative and quantitative one-step analysis of lipids and encapsulated bioactive molecules in liposome preparations by HPTLC/FID (IATROSCAN). J Liposome Res. 2006;16:321–30.
16. Hatziantoniou S, Demetzos C. Method of simultaneous analysis of liposome components using HPTLC/FID. Methods Mol Biol. 2010;606:363–8.
17. Kotanidou A, Loutrari H, Papadomichelakis E, Glynos C, Magkou C, Armaganidis A, *et al.* Inhaled activated protein C attenuates lung injury induced by aerosolized endotoxin in mice. Vasc Pharmacol. 2006;45:134–40.

18. Krump-Konvalinkova V, Bittinger F, Unger RE, Peters K, Lehr HA, Kirkpatrick CJ. Generation of human pulmonary microvascular endothelial cell lines. Lab Invest. 2001;81:1717–27.
19. Psallidas I, Stathopoulos GT, Maniatis NA, Magkouta S, Moschos C, Karabela SP, *et al.* Secreted phosphoprotein-1 directly provokes vascular leakage to foster malignant pleural effusion. Oncogene. 2012. February. [Epub ahead of print].
20. Marik PE. Aspiration syndromes: aspiration pneumonia and pneumonitis. Hosp Pract (Minneap). 2012;38:35–42.
21. Matute-Bello G, Frevert CW, Martin TR. Animal models of acute lung injury. Am J Physiol Lung Cell Mol Physiol. 2008;295:L379–99.
22. Wang Z, Tiruppathi C, Cho J, Minshall RD, Malik AB. Delivery of nanoparticle: complexed drugs across the vascular endothelial barrier *via* caveolae. IUBMB Life. 2011;63:659–67.
23. Oh P, Borgstrom P, Witkiewicz H, Li Y, Borgstrom BJ, Chrastina A, *et al.* Live dynamic imaging of caveolae pumping targeted antibody rapidly and specifically across endothelium in the lung. Nat Biotechnol. 2007;25:327–37.
24. Cohen AW, Hnasko R, Schubert W, Lisanti MP. Role of caveolae and caveolins in health and disease. Physiol Rev. 2004;84(4):1341–79.
25. Suchner U, Katz DP, Furst P, Beck K, Felbinger TW, Senftleben U, *et al.* Effects of intravenous fat emulsions on lung function in patients with acute respiratory distress syndrome or sepsis. Crit Care Med. 2001;29:1569–74.
26. Kalimeris K, Christodoulaki K, Karakitsos P, Batistatou A, Lekka M, Bai M, *et al.* Influence of propofol and volatile anaesthetics on the inflammatory response in the ventilated lung. Acta Anaesthesiol Scand. 2011;55:740–8.
27. Ypsilantis P, Politou M, Mikroulis D, Pitiakoudis M, Lambropoulou M, Tsigalou C, *et al.* Organ toxicity and mortality in propofol-sedated rabbits under prolonged mechanical ventilation. Anesth Analg. 2007;105:155–66.
28. Ott J, Hiesgen C, Mayer K. Lipids in critical care medicine. Prostaglandins Leukot Essent Fat Acids. 2011;85:267–73.